

## Background-Free Observation of Cold Antihydrogen with Field-Ionization Analysis of Its States

G. Gabrielse,<sup>1,\*</sup> N. S. Bowden,<sup>1</sup> P. Oxley,<sup>1</sup> A. Speck,<sup>1</sup> C. H. Storry,<sup>1</sup> J. N. Tan,<sup>1</sup> M. Wessels,<sup>1</sup> D. Grzonka,<sup>2</sup> W. Oelert,<sup>2</sup>  
G. Schepers,<sup>2</sup> T. Seifick,<sup>2</sup> J. Walz,<sup>3</sup> H. Pittner,<sup>4</sup> T. W. Hänsch,<sup>4,5</sup> and E. A. Hessels<sup>6</sup>

(ATRAP Collaboration)

<sup>1</sup>*Department of Physics, Harvard University, Cambridge, Massachusetts 02138*

<sup>2</sup>*IKP, Forschungszentrum Jülich GmbH, 52425 Jülich, Germany*

<sup>3</sup>*CERN, 1211 Geneva 23, Switzerland*

<sup>4</sup>*Max-Planck-Institut für Quantenoptik, Hans-Kopfermann-Strasse 1, 85748 Garching, Germany*

<sup>5</sup>*Ludwig-Maximilians-Universität München, Schellingstrasse 4/III, 80799 München, Germany*

<sup>6</sup>*York University, Department of Physics and Astronomy, Toronto, Ontario, Canada M3J 1P3*

(Received 11 October 2002; published 31 October 2002)

A background-free observation of cold antihydrogen atoms is made using field ionization followed by antiproton storage, a detection method that provides the first experimental information about antihydrogen atomic states. More antihydrogen atoms can be field ionized in an hour than all the antimatter atoms that have been previously reported, and the production rate per incident high energy antiproton is higher than ever observed. The high rate and the high Rydberg states suggest that the antihydrogen is formed via three-body recombination.

DOI: 10.1103/PhysRevLett.89.213401

PACS numbers: 36.10.-k

Antihydrogen ( $\bar{H}$ ) atoms that are cold enough to be trapped for laser spectroscopy [1] promise to provide the most stringent *CPT* tests with baryons and leptons [2], along with more sensitive tests for possible extensions to the standard model [3], building on the high accuracy of hydrogen spectroscopy [4]. It may even be possible to directly observe the gravitational force on antimatter atoms [5].  $\bar{H}$  atoms with a temperature near to the 0.5 K depth of a realistic magnetic trap are greatly preferred since trapping atoms from a thermal distribution is much less likely with increasing temperature.

The ATRAP Collaboration demonstrated the first positron cooling of antiprotons [6,7] in a nested Penning trap [8] more than a year ago. Detailed studies of this cooling (to 4 K) have since been carried out [9] to ensure that the antiproton ( $\bar{p}$ ) loss we observed during positron ( $e^+$ ) cooling corresponds to  $\bar{H}$  formation. This Letter reports an observation of cold  $\bar{H}$  produced during such cooling that is insensitive to other  $\bar{p}$  loss mechanisms. Field ionization of  $\bar{H}$  followed by  $\bar{p}$  storage provides the first experimental information about  $\bar{H}$  excited states. Every recorded event comes from  $\bar{H}$  production, with no background. Another very recent report of cold  $\bar{H}$  formation [10], also during positron cooling in a nested Penning trap, instead identifies  $\bar{p}$  and  $e^+$  annihilations within  $\pm 8$  mm and  $5 \mu\text{s}$  as  $\bar{H}$ , subtracting a background larger than the signal. Observations of high velocity  $\bar{H}$  also used simultaneous annihilation detection [11,12].

More antiprotons from ionized  $\bar{H}$  atoms can now be captured in an hour than the sum of all antimatter atoms reported so far. If the  $\bar{H}$  leave the production region isotropically, then 11% of the  $\bar{p}$  in the nested Penning

trap form  $\bar{H}$ . The  $657 \bar{p}$  we capture from  $\bar{H}$  ionization in the sample used here would then correspond to nearly 170 000 cold  $\bar{H}$  atoms. Even if the distribution is not isotropic, the high rate supports the feasibility of spectroscopic investigations to follow. Rydberg states formed at a high rate likely start with a three-body recombination collision [8] between a  $\bar{p}$  and two  $e^+$ , with deexcitation continuing via other processes [13,14].

The apparatus (Fig. 1) alternates between the one used to demonstrate positron cooling of antiprotons [6] and a close copy. A 5.4 T magnetic field from a superconducting solenoid is directed along the vertical symmetry axis of a stack of gold-plated copper rings. Applied voltages form Penning traps that confine the  $\bar{p}$ ,  $e^-$ , and  $e^+$  and control their interactions. Captured  $\bar{p}$  accumulate in the volume below the rotatable electrode. Above, injected  $e^+$  accumulate simultaneously. The electrodes and surrounding vacuum enclosure are cooled to 4.2 K via a thermal contact to liquid helium. Cryopumping reduces the pressure within the trap to less than  $5 \times 10^{-17}$  Torr, as measured in a similar apparatus [15] using the lifetime of trapped  $\bar{p}$  as a gauge.

All experiments pursuing antihydrogen, and other experiments requiring the lowest energy antiprotons, make use of CERN's unique Antiproton Decelerator (AD). A standard set of techniques that some of us developed over the last 15 years [2] is also used to accumulate cold  $\bar{p}$  in a trap, at an energy that can be more than a factor of  $10^{10}$  times lower than that of  $\bar{p}$  in the AD. Every 100 s, the AD ejects a short pulse of  $\bar{p}$ . The  $\bar{p}$  slow in matter, are captured in a trap that is closed electronically while they are within, and electron cool in the trap to 4.2 K.

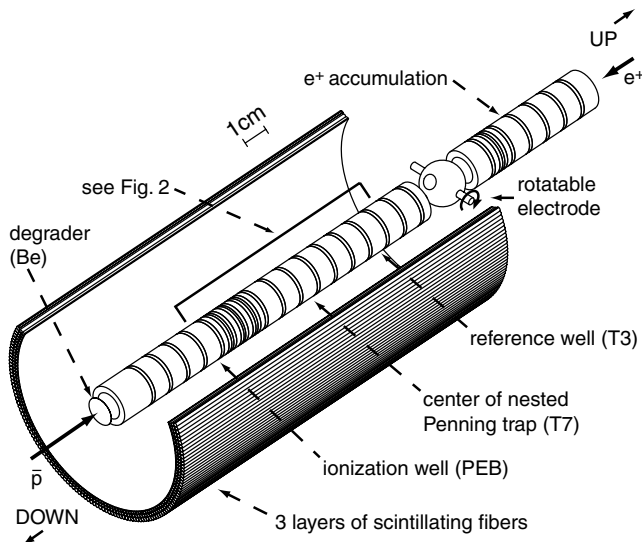


FIG. 1. Overview of the trap and detectors. Antiprotons are loaded from below (left), into the trap electrodes below the rotatable electrode. Positrons are simultaneously loaded from above (right) into the electrodes above the rotatable electrode.  $\bar{\text{H}}$  formation is observed within the lower region detailed in the next figure.

A  $\bar{p}$  stacking technique [16] allows the accumulation of as many  $\bar{p}$  from successive AD pulses as time permits. Typically 150 000 antiprotons end up suspended within electrode T2 [Fig. 2(a)].

The accumulated  $e^+$  [17] originate in a 69 mCi  $^{22}\text{Na}$  source that is lowered through a He dewar to settle against the 4.2 K trap enclosure. Fast  $e^+$  follow magnetic field lines and enter the trap vacuum through a thin Ti window. Some slow as they enter the trapping region through a thin single crystal of tungsten. Others slow while turning around within a thick tungsten crystal that rotates to the trap axis when the rotatable electrode goes to its closed position. Slow  $e^+$  that pick up  $e^-$  while leaving the thin crystal form highly magnetized, Rydberg positronium atoms. These travel parallel to the trap axis until they are ionized by the electric field of a Penning trap well, whereupon the  $e^+$  are captured. With the rotatable electrode in its closed position, neither crystal can be struck by  $\bar{p}$ , thus protecting an essential layer of adsorbed gas on the thin crystal, without which  $e^+$  accumulation ceases [17,18]. With this electrode rotated open,  $e^+$  can be pulsed through and caught in the lower trap region. Particle motions induce detectable currents in resonant  $RLC$  circuits attached to trap electrodes, making it possible to nondestructively detect the  $e^+$  number before and after the transfer. Up to  $1.7 \times 10^6$  cold  $e^+$  are located in electrode T5 [Fig. 2(a)] for these studies.

The nested Penning trap [Figs. 2(a) and 2(b)] is central to the production of cold  $\bar{\text{H}}$ . The  $e^+$  and  $\bar{p}$  have opposite charge signs, and thus cannot be confined or made to interact within the same Penning trap well. Some of us

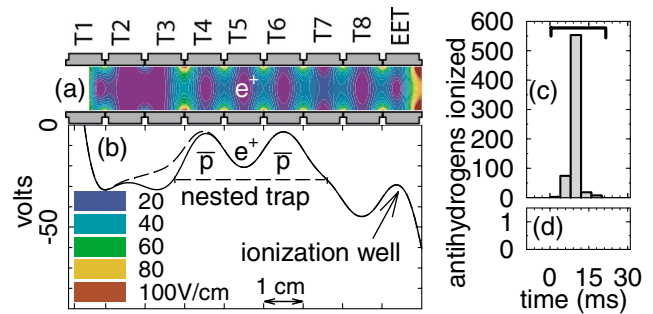


FIG. 2 (color). (a) Electrodes for the nested Penning trap. Inside is a representation of the magnitude of the electric field that strips  $\bar{\text{H}}$  atoms. (b) Potential on axis for positron cooling of antiprotons (solid line) during which  $\bar{\text{H}}$  formation takes place, with the (dashed line) modification used to launch  $\bar{p}$  into the well. (c) Antiprotons from  $\bar{\text{H}}$  ionization are released from the ionization well during a 20 ms time window. (d) No  $\bar{p}$  are counted when no  $e^+$  are in the nested Penning trap.

proposed the nested Penning trap [8], with  $e^+$  within a small inverted well at the center of a larger well for  $\bar{p}$ , as the solution to this challenge. We investigated its properties with  $e^-$  and  $p$  [19], loaded cold  $\bar{p}$  and  $e^+$  together in a nested Penning trap [18], and then used it to observe the positron cooling of antiprotons [6].

To start positron cooling and  $\bar{\text{H}}$  formation, the  $\bar{p}$  are launched into the nested Penning trap by pulsing from the solid to the dashed potential [Fig. 2(b)] for  $1.5 \mu\text{s}$ . The  $\bar{p}$  oscillate back and forth through the cold  $e^+$  within a nearly symmetrical nested Penning trap, restored before the  $\bar{p}$  return to their launch point. They lose energy via collisions with  $e^+$ , which cool via synchrotron radiation to the 4.2 K of their surroundings.

Antihydrogen should form most efficiently when  $e^+$  cool  $\bar{p}$  to the point where the two species have low relative velocities. Upon observing  $\bar{p}$  losses during positron cooling, and intriguing indications of  $\bar{\text{H}}$  production, we undertook a more detailed study of positron cooling [9] to ensure that other mechanisms would not generate signals that could be confused with  $\bar{\text{H}}$  production. The ambipolar diffusion mechanism [20] is particularly troubling since unbound  $e^+$  and  $\bar{p}$  correlate enough to diffuse out of the trap, perhaps even generating simultaneous annihilations of  $\bar{p}$  and  $e^+$ .

Detailed studies of the positron cooling of antiprotons in a nested Penning trap reveal some intricacy, as illustrated with small numbers of  $\bar{p}$  and  $e^+$  in Fig. 3. The average  $\bar{p}$  energy decreases exponentially for short times [Fig. 3(a)], with a time constant that varies with the particle number and density. However, the  $\bar{p}$  energy spectra taken at a sequence of cooling times [Figs. 3(b)–3(e)] reveals a great deal of structure, not yet completely understood. The  $\bar{\text{H}}$  atoms presumably form when the energies of the  $\bar{p}$  (histograms) and  $e^+$  (vertical dashed line) overlap, since their relative velocities are then lowest. On a 10 times longer time scale, the  $\bar{p}$  cool into the side wells

of the nested trap, out of contact with the  $e^+$ . The new cooling mechanism here seems to be a recycled evaporative cooling of the  $\bar{p}$ , whereby hot  $\bar{p}$  that “evaporate” to higher energies in the nested well are cooled by the  $e^+$  before they leave the well. With no  $e^+$  in the nested well, evaporative cooling cools the  $\bar{p}$  on the slower time scale. There is also radial loss of  $\bar{p}$  near the potential maximum at the center of the nested Penning trap.

Any  $\bar{H}$  atom formed is free to move in the initial direction of its  $\bar{p}$ , unconfined by the nested Penning trap.  $\bar{H}$  atoms passing through the field-ionization well in a state that can be ionized by the electric field will leave their  $\bar{p}$  trapped in this well. The ionization well [within electrode EET in Fig. 2(a)] is carefully constructed so that its electric field ensures that no  $\bar{p}$  from the nested Penning trap can get into it (e.g., a  $\bar{p}$  liberated from the nested well by ambipolar diffusion), except if it travels about 4 cm bound within an  $\bar{H}$  atom. Any  $\bar{p}$  heated out of the nested Penning trap escapes over the lower potential barrier in the other direction. Even if a  $\bar{p}$  did acquire enough energy to go over the ionization well in one pass it would not be trapped because there is no mechanism to lower its energy while over this well. In addition, positron cooling lowers the energy of the  $\bar{p}$  in the nested well, taking them farther from the energy required to even pass over the ionization well.

Electric fields [Fig. 2(a)] ionize  $\bar{H}$  Rydberg states. Numerical modeling indicates the capture of  $\bar{p}$  from  $\bar{H}$  atoms that ionize in electric fields between 35 and 95 V/cm. A rough estimate comes from the classical formula [21] for the electric field  $F = 3.2 \times 10^8 n^{-4}$  V/cm that would strip a Rydberg atom entering this field. The binding energy,  $E = 13.6n^{-2}$  eV, defines  $n$  even though it is not a good quantum number in these fields. This suggests the field ionization and capture of  $\bar{p}$  from  $\bar{H}$  atoms with binding energies corresponding to

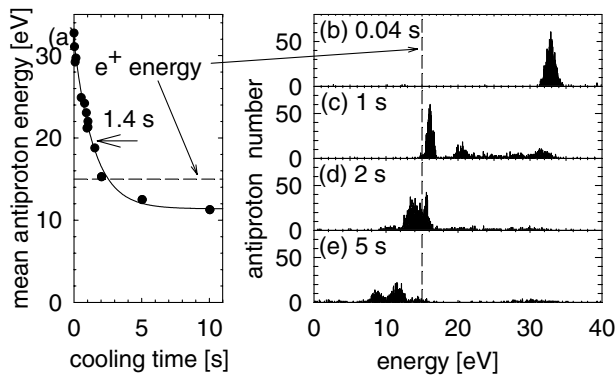


FIG. 3. (a) Antiproton average energy decreases exponentially in time until the antiprotons and positrons have the lowest relative velocity. Cooling then continues but at a 10 times slower rate. (b)–(e) Energy spectra of the  $\bar{p}$  as a function of the positron cooling time. (For this example, 5000  $\bar{p}$  are used, along with 200 000  $e^+$  in a 15 V well.)

$n = 43$  to  $n = 55$ . Refined estimates are needed using methods suited to strong fields.

Only signals from  $\bar{H}$  are detected with this field-ionization method—there is no background at all. Figure 2(c) represents 657 ionized  $\bar{H}$  atoms captured in the ionization well during the course of this experiment—more than all of the  $\bar{H}$  atoms that have been reported so far. In many trials without  $e^+$  we have never seen a single  $\bar{p}$  in the ionization well [Fig. 2(d)]. Antiprotons from  $\bar{H}$  ionization are stored in the ionization well until after positron cooling is completed in the nested well, and all  $e^+$  and  $\bar{p}$  in the nested well are released in the direction away from the ionization well. We then eject the trapped  $\bar{p}$  by ramping down the potential of the ionization well in 20 ms. The ejected  $\bar{p}$  annihilate upon striking electrodes, generating pions and other charged particles that produce light pulses in the scintillators. The ramp is fast enough so that the  $1.2 \text{ s}^{-1}$  cosmic ray background contributes a count in our window only 1 time in 50 in Figs. 2(c) and 2(d). Our experimentally calibrated detection efficiency [22] corresponds to 1 in 2.7 of the stored  $\bar{p}$  producing a coincidence signal in surrounding scintillators.

The number of ionized  $\bar{H}$  atoms increases with the number of  $e^+$  in the nested well [Fig. 4(a)] as might be expected, though this curve is surprisingly insensitive to the total number of  $e^+$  for larger  $e^+$  number. We are exploring some indications that the shape of this measured curve is related to a quadratic dependence of the production rate upon  $e^+$  density. The ionization well can be moved farther away from the center of the nested well, using identical electrodes to the right of EET in Fig. 2(a). The decrease in the number of ionized  $\bar{H}$  [Fig. 4(b)] seems consistent with a quadratic dependence on distance, showing that the  $\bar{H}$  angular distribution is broader than the small solid angle subtended by our ionization well. Isotropic  $\bar{H}$  production and a broad  $\bar{H}$  “beam” along the direction of the magnetic field are both consistent

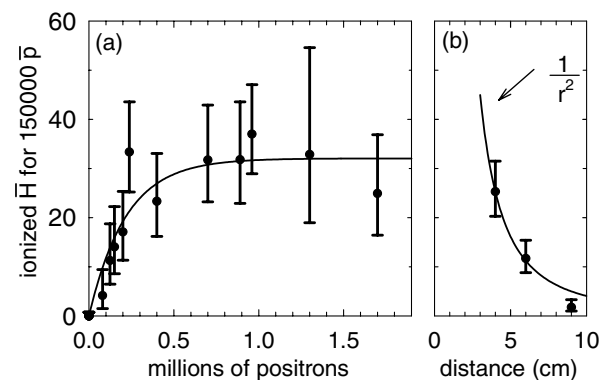


FIG. 4. (a) The number of field-ionized  $\bar{H}$  atoms increases with the number of  $e^+$  in the nested Penning trap of Fig. 2, and then levels off. (b) This number decreases when the ionization well is moved away from the nested Penning trap.

with Fig. 4(b). More study is required to see if the trajectories of the highly polarizable Rydberg atoms could be significantly modified by the electric and magnetic fields.

To give some idea of how efficiently  $\bar{H}$  atoms are stripped and detected we use one trial in which eight AD injection pulses are used to accumulate 148 000 cold  $\bar{p}$ , with 430 000 cold  $e^+$  accumulating simultaneously. After the positron cooling of the antiprotons we determine that 66  $\bar{H}$  atoms have field ionized and left their  $\bar{p}$  in the ionization well. This means that we observe about eight  $\bar{H}$  atoms per AD injection pulse, and about one  $\bar{H}$  atom per 2200 antiprotons in the nested well. (For comparison, smaller values of about 1/4 and 1/12 000 pertain to the very recent implementation of positron cooling of  $\bar{p}$  in a larger trap using more  $e^+$  [10], perhaps because of a higher temperature and a higher background gas pressure.)

If the  $\bar{H}$  production at ATRAP is isotropic, then the 657 ionized  $\bar{H}$  would represent nearly 170 000 cold  $\bar{H}$ . This would mean that a remarkable 11% of the  $\bar{p}$  in the nested Penning trap are forming  $\bar{H}$  atoms — comprising a substantial portion of the large  $\bar{p}$  losses we have been observing during positron cooling of antiprotons since this cooling was first observed. (The ionization well covers only about 1/260 of the total solid angle.)

In conclusion, more  $\bar{H}$  atoms are observed than the sum of all previously reported, and many more are observed per high energy  $\bar{p}$  sent to our apparatus, and per  $\bar{p}$  cooled in our apparatus.  $\bar{H}$  atoms are produced during positron cooling of antiprotons in a nested Penning trap. Improved implementations of such cooling will certainly increase the  $\bar{H}$  production rate. Repeatedly driving  $\bar{p}$  from one side of the nested well to the other with a resonant radio frequency drive, for example, yields 720 ionized  $\bar{H}$  atoms in 1 h [9]. The  $\bar{H}$  signals being observed should allow optimization of techniques and further rate increases.

The electric field ionization of  $\bar{H}$ , followed by  $\bar{p}$  storage until all  $\bar{p}$  losses cease, allows the detection of  $\bar{H}$  atoms without any background at all; only  $\bar{H}$  atoms are observed. The field ionization also gives the first glimpse of  $\bar{H}$  atomic states, with  $n$  roughly between about 43 and 55 here. Changing the ionizing electric field should reveal a more detailed picture and indicate how difficult it may be to deexcite  $\bar{H}$  atoms to states that can be trapped and used for spectroscopic studies. It will be interesting to see if the highly polarizable Rydberg states could be trapped in an electric field minimum for some time, but trapping of  $\bar{H}$  in a magnetic trap superimposed on the Penning traps for charge particles [23] awaits deexcitation of the highly magnetized, highly excited states that have been observed.

We are grateful to CERN, its PS Division and the AD team for delivering the 5.3 MeV antiprotons. This work

was supported by the NSF, AFOSR, the ONR of the U.S., the BMBF, FZ-J, and MPG of Germany, and the NSERC, CRC, and PREA of Canada.

\*ATRAP spokesperson.

Email address: gabrielse@physics.harvard.edu

- [1] G. Gabrielse, in *Fundamental Symmetries*, edited by P. Bloch, P. Paulopoulos, and R. Klapisch (Plenum, New York, 1987), p. 59.
- [2] G. Gabrielse, *Adv. At. Mol. Opt. Phys.* **45**, 1 (2000).
- [3] R. Bluhm, V. A. Kostelecký, and N. Russell, *Phys. Rev. D* **57**, 3932 (1998).
- [4] M. Niering *et al.*, *Phys. Rev. Lett.* **84**, 5496 (2000).
- [5] G. Gabrielse, *Hyperfine Interact.* **44**, 349 (1988).
- [6] G. Gabrielse, J. Estrada, J. N. Tan, P. Yesley, N. S. Bowden, P. Oxley, T. Roach, C. H. Storry, M. Wessels, J. Tan, D. Grzonka, W. Oelert, G. Schepers, T. Sefzick, W. Breunlich, M. Carnegelli, H. Fuhrmann, R. King, R. Ursin, H. Zmeskal, H. Kalinowsky, C. Wesdorp, J. Walz, K. S. E. Eikema, and T. W. Hänsch, *Phys. Lett. B* **507**, 1 (2001).
- [7] In Fig. 6c of the previous reference, the center of the  $e^+$  well should be  $-4$  V. Our current understanding is that recycled evaporative cooling produces the low energy  $\bar{p}$  peak in Fig. 6, while the intermediate energy peak represents  $\bar{p}$  and  $e^+$  with low relative velocities.
- [8] G. Gabrielse, S. L. Rolston, L. Haarsma, and W. Kells, *Phys. Lett. A* **129**, 38 (1988).
- [9] G. Gabrielse *et al.* (to be published).
- [10] M. Amoretti *et al.*, *Nature (London)* **419**, 456 (2002).
- [11] G. Baur *et al.*, *Phys. Lett. B* **368**, 251 (1996).
- [12] G. Blanford *et al.*, *Phys. Rev. Lett.* **80**, 3037 (1998).
- [13] M. Glinsky and T. O'Neil, *Phys. Fluids B* **3**, 1279 (1991).
- [14] P. O. Fedichev, *Phys. Rev. A* **226**, 289 (1997).
- [15] G. Gabrielse, X. Fei, L. A. Orozco, R. L. Tjoelker, J. Haas, H. Kalinowsky, T. A. Trainor, and W. Kells, *Phys. Rev. Lett.* **63**, 1360 (1989).
- [16] G. Gabrielse, N. S. Bowden, P. Oxley, A. Speck, C. H. Storry, J. N. Tan, M. Wessels, D. Grzonka, W. Oelert, G. Schepers, T. Sefzick, J. Walz, H. Pittner, T. W. Hänsch, and E. A. Hessels, *Phys. Lett. A* **548**, 140 (2002).
- [17] J. Estrada, T. Roach, J. N. Tan, P. Yesley, D. S. Hall, and G. Gabrielse, *Phys. Rev. Lett.* **84**, 859 (2000).
- [18] G. Gabrielse, D. S. Hall, T. Roach, P. Yesley, A. Khabbaz, J. Estrada, C. Heimann, and H. Kalinowsky, *Phys. Lett. B* **455**, 311 (1999).
- [19] D. S. Hall and G. Gabrielse, *Phys. Rev. Lett.* **77**, 1962 (1996).
- [20] R. J. Goldston and P. H. Rutherford, *Introduction to Plasma Physics* (IOP, London, 1995).
- [21] T. F. Gallagher, *Rydberg Atoms* (Cambridge, New York, 1994).
- [22] X. Fei, Ph.D. thesis, Harvard University, 1990.
- [23] T. M. Squires, P. Yesley, and G. Gabrielse, *Phys. Rev. Lett.* **86**, 5266 (2001).